the virtualization of cellular base station, mobile core network, home network, and fixed access network, etc. Furthermore, NFV is expected as an innovative technology to promote cost-efficient and new added-value services for satellites [13]. There are already available proposals that combine NC virtualization and software-defined networking (SDN) technology. For example, in [14], the authors investigate the usability of random linear NC as a function in SDNs to be deployed with virtual (software) OpenFlow switches. The NC functions including encoder, re-encoder, and decoder are run on a virtual machine (ClickOS). This work provides a prototype with implementation of additional network functions via virtual machines (VMs) by sharing system resources or additional hardware (e.g. FPGA cards). In [15], NC is implemented in a VM which is then embedded into an Open vSwitch. The paper shows the relation between NC (as a software), VM and host OS of Open vSwich. These works indicate the feasibility of integrating NC as a functionality based on SDN and the concentration of network functions in centralized architectures such as data centers or centralized locations proposed by network operators, service integrators and providers. However, a unified design framework for NC design in view of NFV either centralized or distributed is currently missing. In this paper, we focus on the functional-level design regardless of how it is softwarised.

The motivation of this paper is to show the generalization of NC design domains as a toolbox so that NC can be applied over different operational frameworks and services including satellite or hybrid networks thus enabling softwarization and rapid innovative deployment. Our contributions can be summarized as follows.

- We propose the integration of NC and NFV as a functional architecture given as a structured toolbox of NC design domains so that tailored designs can be implemented in software and deployed over virtualised infrastructures to allow flow engineering tailored to different service operational intent.
- We validate our proposed NC function (NCF) over a complete design for the use case of geo-network coding. VNCF is integrated as a VNF in ETSI NFV architecture. In particular, coding is optimized according to geo-tagged link statistics and geo-location information given the computational complexity constraint. Numerical results indicate that per-link achievable rate region obtained with NC at the source and re-encoding at the intermediate node is twice wider than that of transmission with NC at the source only. Furthermore, connectivity gains up to 32 times and 47 times are obtained if compared with the uncoded case for 80% and 85% target reliability with computational complexity constraint of 125000 operations in terms of multiplications and additions, respectively.

The rest of this paper is organized as follows. In Section 2, we propose the framework of NC design. In Section 3, we validate our proposed architectural design in a specific virtualized Geo-NC function (VGNCF) design using the functionalities identified in previous sections. In Section 4, we conduct numerical results to validate the performance for the case of using our VGNCF design and the uncoded case. Finally, Section 5 identifies conclusions and further work.

## 2. NC DESIGN FRAMEWORK

NFV and NC are two different techniques to address different challenges in the designs of upcoming network technologies. The combination of NFV and NC brings forth a potential solution for the management and operation of the future networks. NC design involves different domains [16]:

- **NC coding domain** - domain for the design of network codebooks, encoding/decoding algorithms, performance benchmarks, appropriate mathematical-to-logic maps, etc.
- **NC functional domain** - domain for the design of the functional properties of NC to match design requirements built upon abstractions of
  - **Network**: by choosing a reference layer in the standardized protocol stacks and logical nodes for NC and re-encoding operations.
  - **System**: by abstracting the underlying physical or functional system at the selected layer e.g. SDN and/or function virtualization.
- **NC protocol domain** - domain for the design of physical signaling/transporting of the information flow across the virtualized physical networks in one way or interactive protocols.

The domain clearly relevant for NC to be designed as a NFV is the NC functional domain and we develop this domain in the next sections.

When interpreting NC as a functionality to the network, NC function virtualization simply consists in integrating the NC architectural framework described above into existing architectural NFV frameworks. As any virtualized network function (VNF), we will also need first of all to identify physical networks/systems infrastructure with the physical computing, storage, and network resources that will provide NC function virtualization (NCFV) with processing, storage, and connectivity through virtualization, respectively.

The architectural integration is proposed here as a toolbox approach. In particular, a set of elementary NC

functionalities are identified that will enable to tailor the use of NC to engineer the throughput and reliability of multiple information network flows depending on the ultimate service operational intent. The resulting VNF will likely operate together with additional virtualized functionalities, which will appropriately be taken care of by the NFV management and orchestration.

Based on the key features of NFV design, our proposed set of basic NC functionalities are distributed into three hierarchical levels based on their significance, universality, and availability. In particular, the common elementary functionalities include NC coding functionalities, NC information flow engineering functionalities, and NC physical/virtualization functions (see [1, 16]).

## 3. Geo-Controlled network connectivity

### 3.1. Physical system/network abstraction

Our interest is to validate the performance of a specific design using the functionalities proposed in the previous sections. In particular, we propose a specific VGNCF design for reliable communication services over satellite, called geo-controlled network connectivity. In the illustrative design proposed here, the optimization functionality will use databases with geo-tagged link statistics and geo-location information of network nodes in the service coverage area for some service operational intents. The overall design target here is to achieve a given connectivity and/or target reliability throughout the service coverage area given constraints of computational complexity.

The interest of NFV is that the same virtualized network functionality can be applied over different operational frameworks and services as well as over different underlying physical networks, including satellite or hybrid networks thus enabling softwarization and rapid innovative deployment. In Fig. 1, we abstract the underlying physical network/system to identify functionalities of NC. All network nodes in the deployment area are geo-localized based on GNSS network. Our proposed use case applies to multiple scenarios consisting of terminals (randomly) distributed in the service area both within and beyond cell coverage of satellites. Connectivity to/from the source is realized via satellites and/or transport networks (e.g. internet, cellular networks), depending on availability but in all cases they are abstracted for our design as sender/sink (end-user) nodes, respectively, through a virtualization layer. Logical network then illustrates information flow functionality of network nodes including encoding, re-encoding, and decoding points.

### 3.2. Virtualized Geo-NC function architecture

Fig. 1 denotes our proposed VGNCF in which we show how NCF can be integrated with the ETSI NFV architecture given the abstracted underlying physical system/network as part of the NFV Infrastructure (NFVI). The design also indicates exchanges between VGNCF and NFV-Management and Orchestration (NFV-MANO) over reference points Ve-Vnfm-Vnf, Nf-Vi, Vi-Vnfm, Or-Vnfm and Or-Vi [17]. Specifically, NFV-MANO is the grey block in Fig. 1 that includes three functional blocks: NFV Orchestrator (NFVO), VNF Manager (VNFM), and Virtualized Infrastructure Manager (VIM). Where NFVO block is considered as the brain of the NFV architecture which has two main responsibilities: (1) the orchestration of NFVI resources across multiple VIMs and (2) the life-cycle management of all network services. While VNFM manages the life-cycle of VNF instances, VIM is responsible for managing and controlling NFVI resources including physical, virtual, and software resources [17].

The detailed functional domain of VGNCF is shown in the VNF block of Fig. 1. At the NC core blocks, interactions with other nodes bring into agreement on coding schemes, coefficients selection, etc. NC coding block receives all inputs such as coding scheme, coefficients, coding parameters, packets from storage block, and signaling to perform elementary encoding/re-encoding/decoding operations, etc. At the NC interoperable blocks, geographical location-based information and level of reliability provided by *geo-controlled reliability* block will be given to the NC optimization and resource allocation block so that optimal coding parameters are generated to the NC coding operation block. In addition, packet loss feedback from other network nodes is also an important factor in the resource allocation process. At the last stage, NC console blocks connect the physical storage and the feedback from other network nodes to provide information packets and packet loss rate to the upper stage, respectively. The proposed NCF will interact with protocol domain, i.e. network, at a suitable position in the reference model of each standardized protocol stack e.g. transportation layer.

As denoted in Fig. 1, NFV-MANO needs the repositories that hold different information regarding network services (NSs) and VNFs (VGNCF is part of VNFs). There are four types of repositories as follows

- **VNF catalogue** represents the repository of all usable VNF packages, supporting the creation and management of the VNF packages.
- **NS catalogue** represents the repository of all usable NSs.
- **NFV instances** is the repository that holds details of all VNF instances and NS instances, represented by either a VNF record or a NS record, respectively.

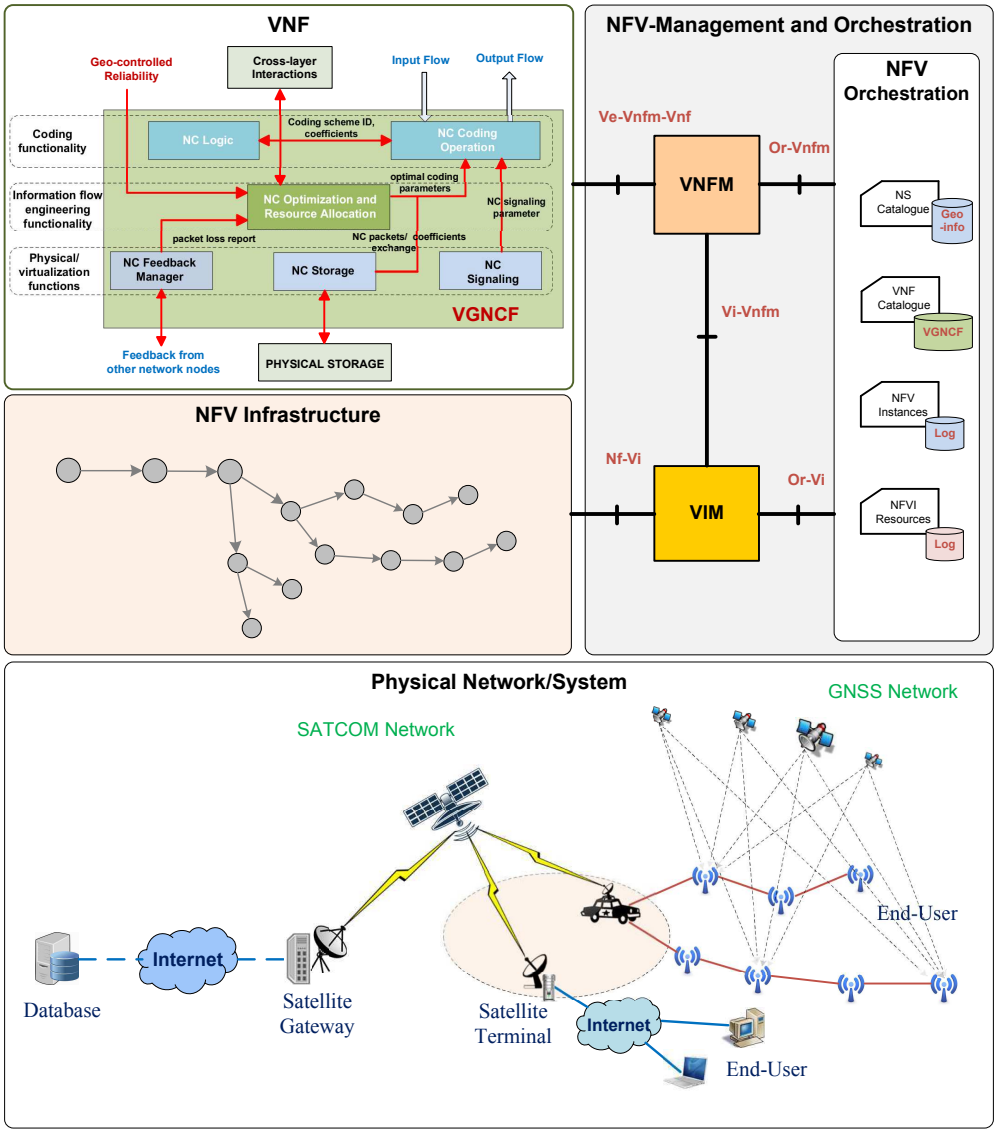


**Figure 1.** VGNCF integrated as a VNF in ETSI NFV architecture.

- **NFVI resources** is the repository that holds information about NFVI resources utilized for the establishment of NS and VNF instances.

## 3.3. Design of Coding Functionality

Let $\epsilon_i$ be the erasure rate of each link $i$ and $\bar{\epsilon}$ be the vector of per-link erasure rates e.g. $\bar{\epsilon} = (\epsilon_1, \epsilon_2)$ for 2 hops. If all links are equal, we use a unique value $\epsilon$. A source generates $n$ coded packets from a set of $k$ information packets over linear map by a coefficient matrix generated using coefficients from the same Galois field of size $g = 2^q$. Then, coding rate is given by $r = k/n$. Assume that packet length is $M$ bits, resulting in $m = M/q$ symbols per packet.

Let $\eta_i(r, \epsilon_i)$ denote the residual erasure rate after decoding at each single hop $i$. The NC codebook will be systematic NC (SNC) as introduced in [18, 19].

In view of multi-hop line networks, we define the reliability after decoding at hop $h$ as

$$\rho_R^{NC}(r, \bar{\epsilon}, h) = \prod_{i=1}^{h} (1 - \eta_i(r, \epsilon_i)) . \quad (1)$$

Accordingly, we define the reliability at hop $h$ for the uncoded case as

$$\rho_R^{noNC}(\bar{\epsilon}, h) = \prod_{i=1}^{h} (1 - \epsilon_i) . \quad (2)$$

## 3.4. Optimization Functionality

**Computational complexity.** Let $\beta_0$ denote the limitation on computational complexity of each node implementing VGNCF. Let $\beta_S(r)$, $\beta_{R_j}(r)$, and $\beta_D(r)$ denote

computational complexity required for NCF at the source, re-encoding points $R_j (1 \leq j < h)$, and the destination, respectively.

**Proposition 1.** The number of multiplications and additions required for encoding process is $N_{enc}^{M} = (n-k)km$ and $N_{enc}^{A} = (n-k)(k-1)m$, respectively. Therefore, computational complexity for encoding in terms of multiplications and additions is $\beta^{enc}(r) = N_{enc}^{M} + N_{enc}^{A} = (n-k)m(2k-1)$. Whereas computational complexity of finite-length decoding complexity using Gaussian Elimination algorithm in terms of the number of multiplications and additions in $GF(2^q)$, denoted by $\beta^{dec}(r) = N_{dec}^{M} + N_{dec}^{A}$, can be found in [20].

Each re-encoding point $j$ will decode and re-encode the linear combinations before forwarding the coded packets towards the next hops. Without decoding the re-encoder does not know which packets are innovative while with decoding the relay may do a more intelligent re-encoding operation. Therefore, the complexity required for the relay is total of computational complexity for decoding and re-encoding, $\beta_{R_j}(r) = \beta^{dec}(r) + \beta^{enc}(r)$. Whereas $\beta_S(r) = \beta^{enc}(r)$ and $\beta_D(r) = \beta^{dec}(r)$. Assume that coding rate $r$ is the same for all the nodes. Then $\beta_S(r)$ is less than $\beta_{R_j}(r)$ and $\beta_D(r)$.

Note that the computational complexity can be equivalently mapped into energy consumption in terms of power per computational unit e.g., logic gates. However, such specification depends on specific hardware that NC function is deployed. As a generalized approach, we thus briefly mention energy consumption via computational complexity in terms of multiplications and additions.

**Utility Function.** Identification of utilities allows the optimization of the network coded flows. We are interested in the design of when NC should be activated in terms of (1) computational complexity/energy consumption and (2) target reliability after decoding ($\rho_0$). In order to do so, we define the following utility function:

$$u^{act}(r, \bar{\epsilon}, \rho_0) = \frac{f^{NC}(r, \bar{\epsilon}, \rho_0)}{f^{COST}(r)}, \tag{3}$$

where $f^{NC}(r, \bar{\epsilon}, \rho_0)$ accounts for the goodness of the encoding/decoding scheme in achieving target performance $\rho_0$. Whereas $f^{COST}(r)$ accounts for the cost in terms of computational complexity. The utility function denotes the energy efficiency in terms of the ratio between the goodness and the computational complexity. We define the goodness and the cost function, respectively, as follows

$$f^{NC}(r, \bar{\epsilon}, \rho_0) = \rho_R^{NC}(r, \bar{\epsilon}) - \rho_0, \tag{4}$$

$$f^{COST}(r) = \beta_S(r), \tag{5}$$

with $\beta_S(r)$ is the computational complexity of the source node as defined in Section 3.4.

**Optimized operative ranges of performance.** The source identifies the upper bound for the energy efficiency of coding strategy and the optimized $\rho_R^{NC}(.)$ that it should provide to the destination according to a given $(\bar{\epsilon}, \rho_0)$ and the computational complexity constraint. Underlying geo-tagged channel statistics are assumed to be stored in NS catalogue (see Fig. 1). The upper bound for energy-efficient coding rate is given by the following proposition.

**Proposition 2.** The source identifies at which rate it maximizes its own utility under constraints of computational complexity by the following optimization strategy:

$$\begin{aligned} \underset{r}{\text{argmax}} \quad & u^{act}(r, \bar{\epsilon}, \rho_0) \\ \text{subject to} \quad & \beta_D(r) \leq \beta_0, \\ & \beta_{R_j}(r) \leq \beta_0. \end{aligned} \tag{6}$$

Numerical results reveal that the utility function has the property of quasi-concavity. Moreover, $\beta_D(r)$ and $\beta_{R_j}(r)$ are increasing functions with redundant coded packets. Therefore, Problem (6) is equivalently quasi-convex optimization and can be efficiently solved by bisection methods [21].

Our proposed strategy identifies optimal points that bring the optimal benefit for the source's viewpoint. It is thus necessary to identify optimized operative ranges of performance so that the destination is aware and admits some variations in the quality. At the source or a centralized controller, the cognitive algorithm to identify optimized operative ranges is briefly realized as follows:

(1) identify maximal utility $u_{max}^{act}(r, \bar{\epsilon}, \rho_0)$ and respective $r$, $\rho_R^{NC}(r, \bar{\epsilon})$ given $(\bar{\epsilon}, \rho_0)$, (2) determine $r$ and $\rho_R^{NC}(r, \bar{\epsilon})$ that satisfies $u_{min}^{act}(.) \leq u^{act}(r, \bar{\epsilon}, \rho_0) \leq u_{max}^{act}(.)$, with $u_{min}^{act}(.)$ is the lower bound, (3) activate the NCF if the range of performance is acceptable by users.

## 4. PERFORMANCE EVALUATION

### 4.1. Per-link achievable rate region

In this section, we indicate that by adding redundancy not only at the source but also at intermediate nodes, per-link achievable rate region goes beyond that of the case that NC is applied only at the source. We consider a single-source multicast network as presented in many communication systems, e.g. a satellite network in which a satellite multicasts information packets to a number of receivers within the service coverage area [22, 23]. Both the uplink and the downlink are erasure channels. We denote the first case as *NC-case* where NCF is applied at both the source and the intermediate node. While the second one is with NC at the source only and known in the NC literature as *end-to-end coding* to which NC can be compared with since the erasure seen by the encoder is the total erasure in the network.

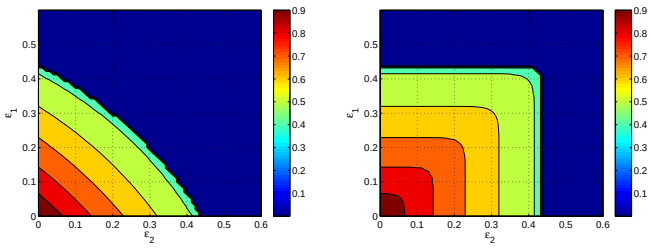

(a) $R^{e2e}$ (b) $R^{NC}$

**Figure 2.** Per-link achievable rate region with respect to link erasure rates for $\eta_0 = 5\%$, $r \in [0.5, 1]$.

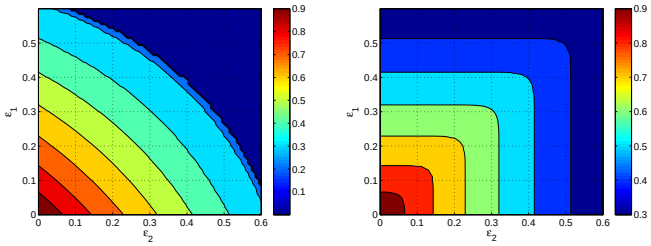

(a) $R^{e2e}$ (b) $R^{NC}$

**Figure 3.** Per-link achievable rate region with respect to link erasure rates for $\eta_0 = 5\%$, $r \in [0.3, 1]$.

It is noted that we use interchangeably the target reliability $\rho_0$ and $\eta_0$, the target residual packet erasure rate after decoding at the receiver, with $\eta_0 = 1 - \rho_0$. Let denote $R^{NC} = r\left(1 - \eta^{NC}\right)$ and $R^{e2e} = r\left(1 - \eta^{e2e}\right)$ as the achievable rate for NC case and end-to-end coding, respectively, where $\eta^{NC}$ is residual erasure rate after decoding for 2-hop networks and $\eta^{e2e}$ corresponds to residual erasure rate after decoding for single-hop networks but with erasure rate is total erasure of the 2-hop network. In the below figures, we show achievable rate region with respect to per-link erasure rates for different target $\eta_0$. First, we consider and analyze the behavior of $R^{e2e}$ and $R^{NC}$ with a limitation of coding rate. We then evaluate the impact of different limitations of coding rate on the behavior of $R^{e2e}$ and $R^{NC}$.

Figure 2 depicts the achievable rate region of the two coding schemes w.r.t. various values of link erasure rates for different $\eta_0$ with $\eta_0 = 5\%$, where coding rate is limited in range from 0.5 to 1. For each value of $(\epsilon_1, \epsilon_2)$, we choose a coding rate as large as possible so that $\eta^{e2e}$ and $\eta^{NC}$ satisfy $\eta_0$, respectively with end-to-end coding and coding at the source and re-encoding at the intermediate node. We term achievable region as the region where $\eta_0$ is satisfied. Otherwise, the region in blue represents the cases in which there is not any coding rate in the given range that meets $\eta_0$.

As denoted in Fig. 2a, $R^{e2e}$ reaches 0.9 since channel condition is good. However, since link erasure rates increase, respective regions such as red, orange, etc show the reduced $R^{e2e}$. This is due to lower coding rate required to meet $\eta_0$ in worse channel conditions. It is interesting to note that each region is shaped by curves. On the other hand, Fig. 2b denotes $R^{NC}$ w.r.t. link erasure rates where achievable regions are shaped by squares. In general, coding at the source and re-encoding at the intermediate node can widen the achievable region to approximately 90% if compared to end-to-end coding. The detailed proof can be seen in Appendix.

In addition, in Fig. 3, regions of $R^{e2e}$ and $R^{NC}$ have been extended by appearance of some new regions located at points with higher $\epsilon_i$ $(i = 1, 2)$ if compared with those of Figure 2. Main reason is that with a wider range of coding rate, regions with very bad channel conditions which $\eta_0$ cannot be satisfied by any $r \in [0.5, 1]$ are now covered due to a wider range of feasible coding rate.

In general, we can conclude that

- The shapes of $R^{e2e}$ and $R^{NC}$ are curves and squares, respectively, regardless the constraints of $r$ and $\eta_0$. The difference is the extension of achievable rate region when a wider range of coding rate is allowable.
- Achievable rate region obtained with NC case is almost twice wider than that of end-to-end coding for the same limitation of coding rate and $\eta_0$.
- The shapes of $R^{NC}$ and $R^{e2e}$ are symmetric over the diagonal. Therefore, $R^{NC}$ and $R^{e2e}$ are independent of the order of the two links.

Our results indicate that NC at the source and re-encoding at the intermediate nodes can enhance significantly network performance in terms of achievable rate. Therefore, we will apply NC whenever an intermediate node is ready to implement NCF. For the latter, in the specific application of geo-controlled network connectivity, we evaluate the optimized utility, reliability, and connectivity gain beyond the service coverage area of satellite with assumption that NC is deployed both at the source and intermediate nodes along the path.

## 4.2. Geo-controlled network connectivity

In this section, we evaluate the reliability and connectivity gain for the case of using our design of VGNCF with respect to the number of hops for communication services beyond the coverage area of satellite in low and high complexity constraints. Databases with geo-tagged link statistics and geo-location information are utilized for the optimization functionality towards the efficient use of network

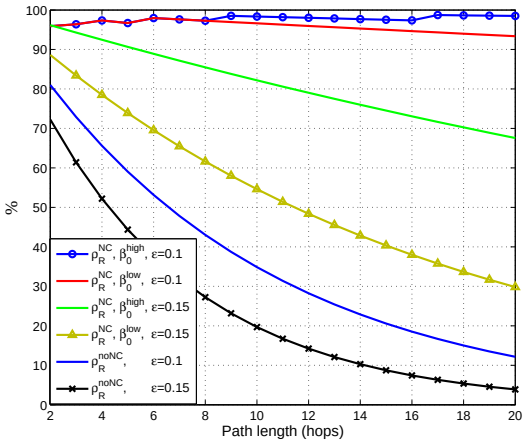


**Figure 4.** Reliability with NC, $\rho_R^{NC}$, and uncoded case, $\rho_R^{noNC}$, according to optimized utility respectively for different path length and erasure rates, with $\rho_0 = 80\%$.

resources. The proposed solution can cope with technical problems such as providing transmission to devices at low power locations (e.g. long distance and/or obstacles) or to extend the transmission beyond the coverage of satellite. We evaluate the potential of our solution through simulation results using Matlab.

For illustrative purposes, we assume that a great number of network devices are uniformly distributed in the deployment area. All links undergo the same erasure rate for different cases of $\epsilon = 0.1$ and 0.15, while $k = 50$ information packets, $M = 100$ bytes, $q = 8$, $\rho_0 = 80\%$ for two different computational complexity constraints, $\beta_0^{low} = 125000$ and $\beta_0^{high} = 150000$ operations. Coding rate is optimized according to Section 3.4.

**Network Reliability.** We conduct various numerical results to evaluate how network performance will be improved with VGNCF according to system limitations and different network conditions such as erasure rate, path length, etc.

A glance at Fig. 4 reveals that network reliability with NCF outperforms the case of transmission without NC. Note that we only denote the path length up to 20 hops in which the performance of the no-NC case is extremely low and thus 20 hops are large enough for our comparison. In particular, $\beta_0^{high}$ can guarantee the target $\rho_0 = 80\%$ for a path length of more than 20 hops (even some hundred hops) in low erasure rate. For longer paths, the NCF just needs to increase the redundant level of combined packets in order to cope with the residual erasure rate. In comparison with NC case, network performance without NC (no-NC case) degrades dramatically with the number of hops. Especially, consider such high complexity constraints, the target is only satisfied up to approximately 12 hops in bad conditions e.g. $\epsilon = 0.15$. The reason is that the longer the transmission path, the lower the connectivity due to physical limits. The limitations of redundant combined packets then cannot provide the packet successfully-received after decoding as the design target.

As we have seen, the target reliability can be satisfied for different erasure rates depending on the redundancy of coded packets generated by the source, i.e. some computational cost is needed for activating NCF and thus equivalently requiring more energy consumption at network nodes.

**Connectivity gain.** Assuming some reliability design target $\rho_0$, in the uncoded case, many nodes would not achieve the target $\rho_0$ while NC case could. Let $h^{NC}(\rho_0)$ and $h^{noNC}(\rho_0)$ denote the hop at which NC and the uncoded case can provide connectivity with the reliability satisfying $\rho_0$, respectively. For simplicity, the connectivity gain for a target $\rho_0$ is defined as $\gamma(\rho_0) = h^{NC}(\rho_0)/h^{noNC}(\rho_0)$.

Fig. 5 depicts connectivity gain when using NCF in times for different $\rho_0$ with $\beta_0^{very-low} = 100000$, $\beta_0^{low} = 125000$, and $\beta_0^{high} = 150000$. The larger the computational constraint, the higher the connectivity gain beyond the cell coverage of the satellite. Particularly, since $\epsilon = 0.1$, NC can obtain up to 335 times and 495 times gain in connectivity if compared to the uncoded case with high constraint for 80% and 85% target reliability, respectively. Otherwise, in low constraint, the connectivity gain obtained with NC is 32 times and 47 times for 80% and 85% reliability, respectively. The reason is that the performance of the uncoded case is significantly impacted by per-link erasure rate and length of transmission path. NC case, meanwhile, can adapt its coding rate within the constraints to obtain the target reliability while optimizing the source's utility. However, implementing NCF is then strongly affected by computational complexity which is equivalently mapped into the cost of energy consumption.

## 5. Conclusions

In this paper, we have proposed the integration of NC and NFV architectural design. Particularly, NC functionalities have been identified as a toolbox so that NC can be designed as a virtual network function thus providing flow engineering functionalities to the network. We have conducted a complete design to illustrate the use and relevance of our proposed VGNCF design where geographical information is the key enabler to support VGNCF. Especially, optimization functionality ensures an optimized and energy-efficient operation of VGNCF. Extensive numerical results show the improvement of overall throughput (achievable rate) with NC at the source and re-encoding at the intermediate nodes if compared with transmission with NC at the source only. Furthermore, the service-driven optimized VGNCF

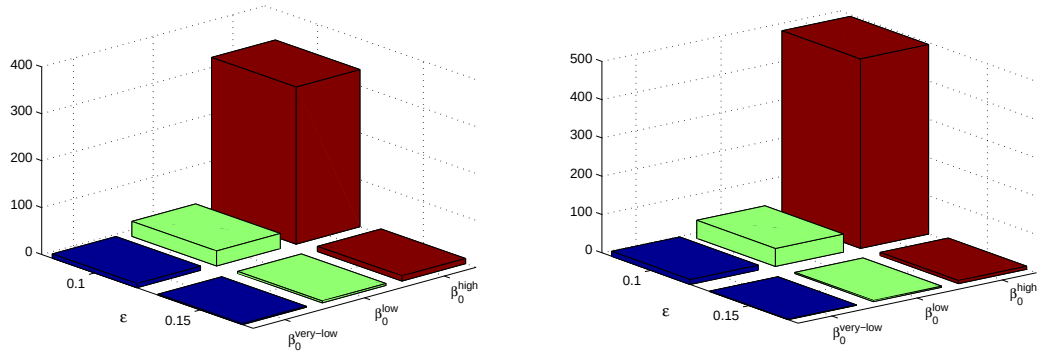


**(a)** $\rho_0 = 80\%$ **(b)** $\rho_0 = 85\%$

**Figure 5.** Connectivity gain according to the optimized NC (in times) for different $\rho_0$ and $\beta_0$.

can provide connectivity gain up to 32 times and 47 times in comparison with the uncoded case for 80% and 85% reliability with complexity constraint of 125000 operations.

Our proposed framework can naturally be tailored for different designs and accommodate additional functionalities. Moreover, the proposed architectural design framework and interaction between VGNCF and NFV-MANO functional blocks can also be generalized as a design framework for several different VNFs.

$\eta^{e2e}$ depends on end-to-end packet erasure rate given as $\eta^{e2e} = 1-(1-\epsilon_1)(1-\epsilon_2)$. $\eta^{e2e}$ and $R^{e2e}$ thus directly depend on the product $(1-\epsilon_1)(1-\epsilon_2)$. Therefore, we will consider whether there exists a set of $(\epsilon_1, \epsilon_2)$ with the same value of the product $(1-\epsilon_1)(1-\epsilon_2)$ leading the same $R^{e2e}$.

We evaluate the function $f(\epsilon_1, \epsilon_2) = (1-\epsilon_1)(1-\epsilon_2)$ to address the existence of such set of $(\epsilon_1, \epsilon_2)$ and how they affect the shapes of $R^{e2e}$ as depicted in Figures 2a-3a.

We assume that there is a set of $(\epsilon_1, \epsilon_2)$ so that $f(\epsilon_1, \epsilon_2)$ is a given constant, e.g. $(1-\epsilon_1)(1-\epsilon_2) = A$, for some $(\epsilon_1, \epsilon_2)$ in a limited range e.g. $\epsilon_i \in [0, 0.6]$ $(i = 1, 2)$. For example, for $(\epsilon_1 = a, \epsilon_2 = 0)$, we find $f(\epsilon_1 = a, \epsilon_2 = 0) = A$. Then, our concern is that whether there is a set of $(\epsilon_1, \epsilon_2)$ so that value of the product $f(\epsilon_1, \epsilon_2)$ is still equal to $A$. If $(1-\epsilon_1)(1-\epsilon_2) = A$ and an arbitrary $\epsilon_1$, it necessarily exists $\epsilon_2$ written by

$$\epsilon_2 = f(\epsilon_1) = \frac{\epsilon_1 + A - 1}{\epsilon_1 - 1}. \tag{E.1}$$

Note that the point $(\epsilon_1 = a, \epsilon_2 = 0)$ satisfies Eq. E.1 and there are infinitely such points. Analyzing Equation E.1, a form of reciprocal graphs, we obtain numerical results as denoted in Fig. E.1.

Assume that $\epsilon_1 \in [0, 0.6]$, $\epsilon_2 \in [0, 0.6]$, we find some values of $A$ respectively to some points of $(\epsilon_1 = a, \epsilon_2 = 0)$, e.g. $(\epsilon_1 = 0.5, \epsilon_2 = 0)$, $(\epsilon_1 = 0.4, \epsilon_2 = 0)$, $(\epsilon_1 = 0.3, \epsilon_2 = 0)$, $(\epsilon_1 = 0.2, \epsilon_2 = 0)$, $(\epsilon_1 = 0.1, \epsilon_2 = 0)$. As depicted in Fig. E.1, it is interesting to see that

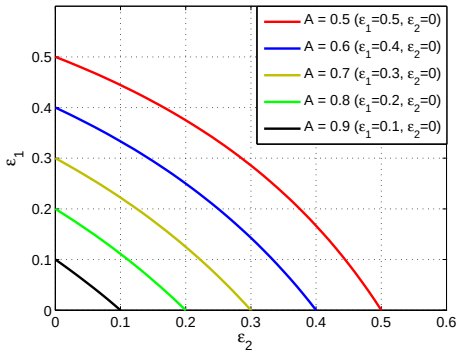


**Figure E.1.** Illustration of some values of $(\epsilon_1, \epsilon_2)$ that brings the same $R^{e2e}$.

(1) There exists a set of $(\epsilon_1, \epsilon_2)$ for a specific constant $A$ respectively to a point $(\epsilon_1 = a, \epsilon_2 = 0)$.

(2) The set of $(\epsilon_1, \epsilon_2)$ with respect to $A$ draws a symmetric curve. In other words, this proves the existence of a set of $(\epsilon_1, \epsilon_2)$ producing a same value of $(\epsilon_1, \epsilon_2)$ and therefore, $R^{e2e}$ obtains a same value for the set of $(\epsilon_1, \epsilon_2)$.

(3) The above results also indicate the symmetry of the curves and the independence of the order of the links. Especially, it is clear to observe the shapes of regions at the frontier and at the boundary of achievable rate region as shown in Figures 2a-3a. Furthermore, as for small values of $(\epsilon_1, \epsilon_2)$, the curves look as lines within our limitation of $(\epsilon_1, \epsilon_2)$.

**Acknowledgement.** The paper has been presented in part at the 2016 IEEE 17th International Workshop on Signal Processing Advances in Wireless Communications (SPAWC),

Edinburgh, UK [1] and in part at the 2017 IEEE International Conference on Communications (ICC), Paris, France [2].

## References


[1] D.-D. Tan and M. A. Vazquez-Castro, "Network coding function virtualization," in *2016 IEEE 17th International Workshop on Signal Processing Advances in Wireless Communications (SPAWC)*, pp. 1–5, July 2016.

[2] D.-D. Tan and M. A. Vazquez-Castro, "Geo-network coding function virtualization for reliable communication over satellite," in *2017 IEEE International Conference on Communications (ICC)*, pp. 1–6, 2017.

[3] R. Ahlswede, N. Cai, S. Y. R. Li, and R. W. Yeung, "Network information flow," *IEEE Transactions on Information Theory*, vol. 46, no. 4, pp. 1204–1216, 2000.

[4] A. F. Dana, R. Gowaikar, R. Palanki, B. Hassibi, and M. Effros, "Capacity of wireless erasure networks," *IEEE Transactions on Information Theory*, vol. 52, pp. 789–804, Mar. 2006.

[5] A. U. Rehman, R. L. Aguiar, and J. P. Barraca, "Network functions virtualization: The long road to commercial deployments," *IEEE Access*, vol. 7, pp. 60439–60464, 2019.

[6] R. Mijumbi, J. Serrat, J. L. Gorricho, N. Bouten, F. D. Turck, and R. Boutaba, "Network function virtualization: State-of-the-art and research challenges," *IEEE Communications Surveys Tutorials*, vol. 18, no. 1, pp. 236–262, 2016.

[7] B. Han, V. Gopalakrishnan, L. Ji, and S. Lee, "Network function virtualization: Challenges and opportunities for innovations," *IEEE Communications Magazine*, vol. 53, no. 2, pp. 90–97, 2015.

[8] C. Liang and F. R. Yu, "Wireless network virtualization: A survey, some research issues and challenges," *IEEE Communications Surveys Tutorials*, vol. 17, no. 1, pp. 358–380, 2015.

[9] I. Afolabi, T. Taleb, K. Samdanis, A. Ksentini, and H. Flinck, "Network slicing and softwarization: A survey on principles, enabling technologies, and solutions," *IEEE Communications Surveys Tutorials*, vol. 20, no. 3, pp. 2429–2453, 2018.

[10] M. Fallgren and B. T. (Eds.), "Scenarios, requirements and kpis for 5g mobile and wireless system," in *ICT-317669-METIS/D1.1*, 2013.

[11] A. Gupta and R. K. Jha, "A survey of 5g network: Architecture and emerging technologies," *IEEE Access*, vol. 3, pp. 1206–1232, 2015.

[12] The European Telecommunications Standards Institute, "Network functions virtualisation (NFV); use cases," in *GS NFV 001 (V1.1.1)*, Oct. 2013.

[13] G. Gardikis, S. Costicoglou, H. Koumaras, C. Sakkas, A. Kourtis, F. Arnal, L. M. Contreras, P. A. Gutierrez, and M. Guta, "Nfv applicability and use cases in satellite networks," in *2016 European Conference on Networks and Communications (EuCNC)*, pp. 47–51, 2016.

[14] D. Szabo, F. Nemeth, B. Sonkoly, A. Gulyas, and F. H. Fitzek, "Towards the 5G revolution: A software defined network architecture exploiting network coding as a service," *SIGCOMM Comput. Commun. Rev.*, vol. 45, no. 4, pp. 105–106, 2015.

[15] J. Hansen, D. Lucani, J. Krigslund, M. Medard, and F. Fitzek, "Network coded software defined networking: enabling 5G transmission and storage networks," *Communications Magazine, IEEE*, vol. 53, no. 9, pp. 100–107, 2015.

[16] M. A. Vazquez-Castro and P. Saxena, "Network coding over satellite: From theory to design and performance," in *Volume 154 of the series Lecture Notes of the Institute for Computer Sciences, Social Informatics and Telecommunications Engineering*, pp. 315–327, Sept. 2015.

[17] The European Telecommunications Standards Institute, "Network functions virtualisation (nfv); management and orchestration," in *ETSI GS NFV-MAN 001 V1.1.1*, Dec. 2014.

[18] B. Shrader and N. Jones, "Systematic wireless network coding," in *Military Communications Conference, 2009. MILCOM 2009. IEEE*, pp. 1–7, 2009.

[19] S. Wunderlich, F. Gabriel, S. Pandi, F. H. P. Fitzek, and M. Reisslein, "Caterpillar RLNC (CRLNC): A practical finite sliding window rlnc approach," *IEEE Access*, vol. 5, no. 99, pp. 20183–20197, 2017.

[20] G. Garrammone, "On decoding complexity of reed-solomon codes on the packet erasure channel," *IEEE Communications Letters*, vol. 17, no. 4, pp. 773–776, 2013.

[21] S. Boyd and L. Vandenberghe, *Convex Optimization*. Cambridge University Press, 2004.

[22] D.-D. Tan and M. A. Vazquez-Castro, "Efficient communication over cellular networks with network coding in emergency scenarios," in *2015 2nd International Conference on Information and Communication Technologies for Disaster Management (ICT-DM)*, pp. 71–78, 2015.

[23] M. A. Vazquez-Castro, P. Saxena, D.-D. Tan, T. Vamstad, and H. Skinnemoen, "SatNetCode: Functional design and experimental validation of network coding over satellite," in *the International Symposium on Networks, Computers and Communications (ISNCC)*, 2018.